European Review for Medical and Pharmacological Sciences 2021; 25: 487-497

Identification of the pivotal differentially expressed genes and pathways involved in *Staphylococcus aureus*-induced infective endocarditis by using bioinformatics analysis

S.-J. XIAO[1], Y.-F. ZHOU[3], H. JIA[2], Q. WU[1], D.-F. PAN[1]

[1]Department of Cardiology, The Affiliated Hospital of Xuzhou Medical University, Xuzhou, Jiangsu, China
[2]Department of Neurosurgery, The Affiliated Hospital of Xuzhou Medical University, Xuzhou, Jiangsu, China
[3]Department of Cardiology, The First Affiliated Hospital of Nanjing Medical University, Nanjing, Jiangsu, China

Abstract. – OBJECTIVE: Infective endocarditis (IE), particularly by *Staphylococcus aureus*, is an uncommon bacteremia-associated infection of the endocardium and cardiac valves. Herein, we evaluated predictive noninvasive biomarkers for IE caused by *S. aureus* through bioinformatics analysis.

MATERIALS AND METHODS: *Staphylococcus aureus*-associated and IE-associated differentially expressed genes (DEGs) were identified by bioinformatics analysis of the GSE6269 and GSE29161 Gene Expression Omnibus (GEO) datasets. The DEGs were analyzed with the LIMMA package, and the coregulated genes were chosen as the intersection of DEGs between the two datasets, called common differentially expressed genes (CDEGs). The enrichment study of CDEGs was subsequently performed with the DAVID and KOBAS web resources. Finally, protein-protein interaction (PPI) network, microRNA (miRNA)-transcription factor (TF)-mRNA (messenger RNA) regulatory network, and the network of drug-genes were identified.

RESULTS: From GSE6269 and GSE29161, respectively, a total of 201 and 741 DEGs were obtained. Gene Ontology (GO) analysis showed that CDEGs were primarily involved in innate immune response, extracellular exosome, as well as calcium ion binding, while the pathway analysis of Kyoto Encyclopedia of Genes and Genomes (KEGG) revealed that CDEGs were significantly enriched in the B-cell receptor, IL-17, and NF-kappa B signaling pathways. The hub genes in the PPI network included HP, S100A12, SPI1, CD14, CCR1, S100A9 and so on. In the miRNA-TF-mRNA regulatory network, SPI1 could target miR-361-5p, miR-155-5p, and miR-339-5p in the progression of IE.

CONCLUSIONS: Several pivotal genes and pathways were identified in the progression of *S. aureus*-induced IE, which may have the potential for early detection.

Key Words:
Staphylococcus aureus, Infective endocarditis, Differentially expressed genes, Pathways, Protein-protein interaction network, MicroRNA-transcription factor-mRNA network.

Introduction

Infective endocarditis (IE) is a severe, mostly bacterial disease with an occurrence of 1.7–10/100 000 person-years, defined as an infection of a native or prosthetic heart valve, the endocardial surface, or an indwelling cardiac device[1,2]. IE is linked to serious complications and high rates of in-hospital mortality, despite advances in medicine[3]. *Staphylococcus aureus* can cause both acute and recurrent persistent infections and is a frequent cause of IE[4]. Early diagnosis of IE is currently challenging. Echocardiography remains the primary imaging test for IE, but it is skipped in up to 30% of cases[5]. The possibility of IE should be considered in all patients with gram-positive bacteremia, especially due to *S. aureus*[6]. However, the mechanisms of *S. aureus*-induced IE are poorly known.

Current research has concentrated on the mechanisms of *S. aureus* infection. Phagocytosis by neutrophils and macrophages is the main mechanism through which *S. aureus* in-

Corresponding Author: Defeng Pan, Ph.D; e-mail: xzdefengpan@yahoo.com and xb@xzhmu.edu.cn

fection is regulated by the immune system[7]. In addition, miRNAs, including miR-142, miR-24, miR-223 and miR-155, play an important role in immune defense toward *S. aureus* infections by modulating a wide variety of events such as inflammatory reactions, host innate immunity, and adaptive immunity[8]. Ranganathan et al[9] found that the general stress response of *S. aureus* might be conducive to the development of chronic infection by acting on host immune defenses. Nonetheless, few studies have attempted to determine the mechanism of *S. aureus* infection-induced IE.

Bioinformatics is the science of storing, extracting, and analyzing biological information by using computers as tools[10]. In terms of biomarker discovery, the rapid development of bioinformatics has provided a popular and feasible means of studying diseases[11]. In the present study, by analyzing the microarray data of *S. aureus* infection and IE in the Gene Expression Omnibus (GEO) public database, we screened out the differentially expressed genes (DEGs), conducted Gene Oncology (GO) enrichment analysis and Kyoto Encyclopedia of Genes and Genomes (KEGG) pathway analysis, analyzed protein-protein interaction (PPI) network, and constructed microRNA (miRNA)-transcription factor (TF)-mRNA (messenger RNA) network and drug-gene network to identify key genes and pathways that participated in *S. aureus*-induced IE. Not only do these results provide novel insights into the disease mechanisms but they also provide new therapeutic targets that can help to establish more effective *S. aureus*-induced IE treatments.

Materials and Methods

Microarray Data

The microarray expression data of GSE6269 and GSE29161 were acquired from the GEO database (https://www.ncbi.nlm.nih.gov/geo/)[12] and were selected for DEG analysis. The dataset GSE6269 included 31 samples from the blood leukocytes of pediatric patients with *S. aureus* infection and six unrelated healthy controls based on the platform Affymetrix Human Genome U133 Array. A further of five IE patients and five healthy control samples were collected from the GSE29161 dataset, which was sequenced by Agilent-014850 Whole Human Genome Microarray 4x44K G4112F.

Screening of DEGs

The raw microarray data of the two datasets was processed using the R language LIMMA package to filter the DEGs[13]. Probe sets without corresponding gene symbols or genes with over one probe set were omitted or averaged, respectively. The criteria of p-value <0.05 and | log2(-fold change, FC) | >1 parameter were set as the cut-off values for DEG screening.

GO and KEGG Enrichment Analyses of Common DEGs

To analyze the function of common DEGs (CDEGs), GO annotation and KEGG pathway enrichment analyses of the CDEGs were performed using the Database for Annotation, Visualization and Integrated Discovery (DAVID, https://david.ncifcrf.gov/)[14] and KOBAS 3.0 (http://kobas.cbi.pku.edu.cn) webtool[15], respectively. The significantly enriched GO terms and KEGG pathways met the criterion of p <0.05 and counts ≥ 2.

PPI Network Analysis

The Search Tool for Retrieving Interacting Genes/Proteins (STRING) database (https://string-db.org/)[16] was used to predict the association between CDEGs, and the PPI network was constructed by Cytoscape[17]. Disconnected nodes in the network were removed to achieve precise results.

MicroRNA (miRNA)-Transcription Factor (TF)-mRNA (messenger RNA) Regulatory Network Analysis

Target miRNAs of CDEGs were predicted by the intersection of the result of miRTarbase (http://starbase.sysu.edu.cn/)[18] and StarBase (http://starbase.sysu.edu.cn/)[19] to improve the accuracy of prediction. The pairs of miRNAs and mRNAs were acquired. The CDEGs were subsequently uploaded to the Enrichr database (http://amp.pharm.mssm.edu/Enrichr/)[20], and the TFs targeting the CDEGs were predicted. A p-value of <0.05 was selected to screen the predicted TFs. Finally, the miRNA-TF-mRNA regulatory relationships were visualized with Cytoscape.

Drug-Gene Network Analysis

The drug-gene interaction database (DGIdb, www.dgidb.org) is a web resource that consolidates, organizes, and presents drug-gene interactions and gene druggability information from papers, databases, and web resources[21]. With the

help of the DGIdb database, drug-gene pairs were predicted for the CDEGs. Finally, the drug-gene network was built by Cytoscape.

Statistical Analysis

A value of p <0.05 was considered significant.

Results

Identification of DEGs

A total of 201 DEGs (148 upregulated and 53 downregulated) and 741 DEGs (349 upregulated and 392 downregulated) were identified from the GSE6269 and GSE29161, respectively (Figures 1A and 1B). Venn diagrams showed that there were 36 co-regulated genes, including 30 co-up-regulated genes and six co-downregulated genes, in the two datasets (Figure 1C). The detailed information concerning CDEGs is listed in Table I. The heat map of the CDEGs is shown in Figure 2.

Functional Analyses of Common DEGs

According to a threshold of p <0.05 and count ≥2, we conducted GO functional enrichment analysis on the CDEGs. CDEGs were enriched in 12 Biological Process (BPs), including innate immune response, defense response to bacterium, antibacterial humoral response, inflammatory response, and immune response. For the Cell Component (CC), the CDEGs were enriched in extracellular exosome and integral component of the plasma membrane. Analysis of molecular function (MF) suggested that the CDEGs were mainly enriched in peptidoglycan receptor activity and RAGE receptor binding (**Supplementary Table I**). The KEGG pathway analysis showed that the CDEGs were significantly enriched in the B-cell receptor signaling, IL-17 signaling, NF-kappa B signaling, and cAMP signaling pathways (Figure 3 and (**Supplementary Table II**).

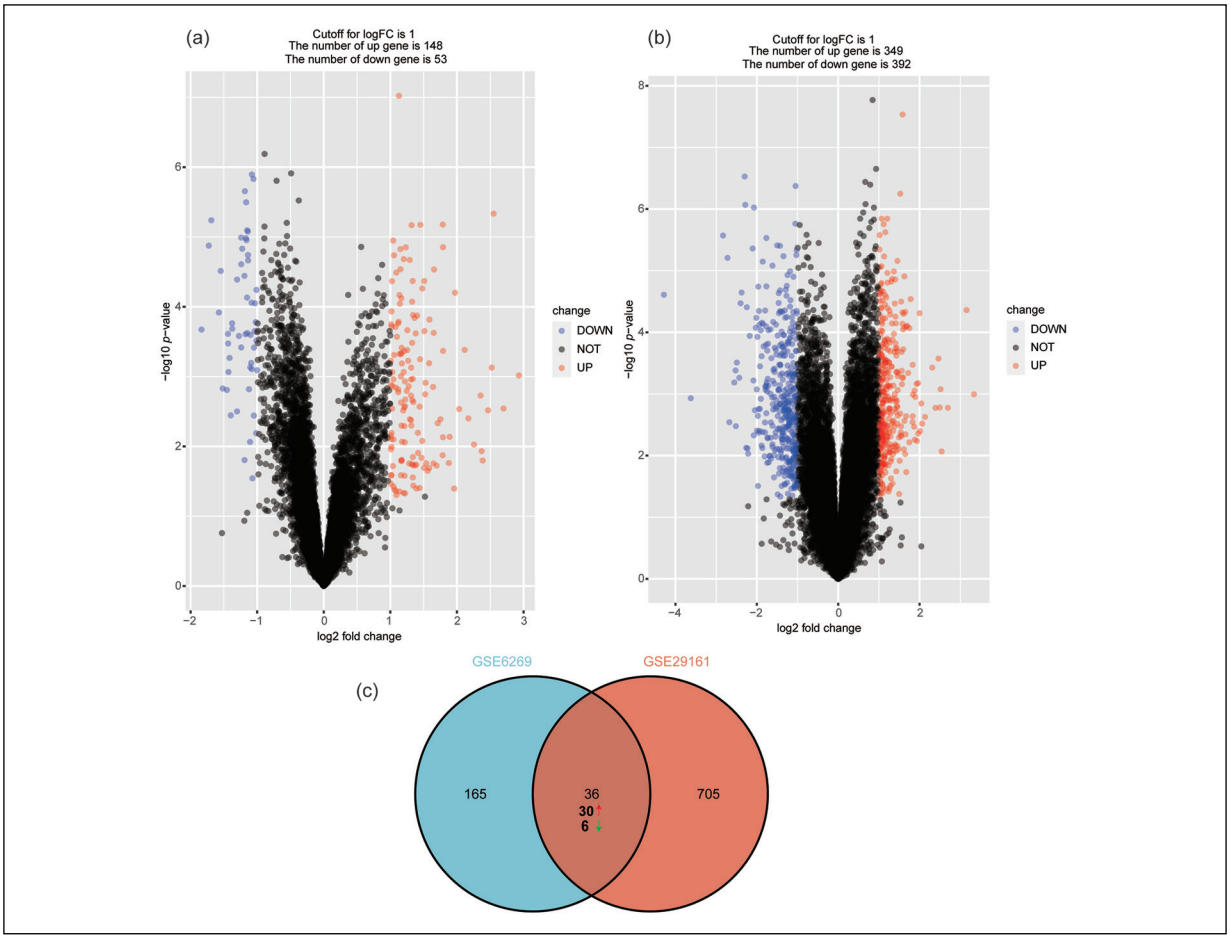

Figure 1. Volcano plots and Venn diagram of DEGs. **A,** and **B,** Volcano plots of GSE6269 and GSE29161. Red plot points represent up-regulated DEGs and blue plot points represent down-regulated DEGs. **C,** Venn diagram shows the common DEGs between the GSE6269 and GSE29161 databases. Abbreviations: DEGs, differentially expressed genes; FC, fold change.

Table I. The common differentially expressed genes screened from GSE6269 and GSE29161.

Common genes	GSE6269		GSE29161	
	logFC	*p*-value	logFC	*p*-value
ADM	2.55165006	4.64E-06	1.10444436	0.033522835
RNASE2	2.115852446	0.000414652	1.23335666	0.014332187
MYL9	2.034585646	0.002915536	1.09116582	0.029766135
FCGR1B	1.971084044	6.28E-05	2.51512366	0.000837472
S100A12	1.791895795	0.000428898	2.04168434	0.00142879
ANXA3	1.789231136	0.007384978	1.654239	0.004518276
ANPEP	1.787403744	6.64E-06	1.03919068	0.01832919
G0S2	1.646659387	0.017502448	1.24106167	0.038243077
MXD1	1.480058129	5.47E-05	1.0670285	0.004854455
HP	1.468772161	0.014590253	1.61278731	0.007905672
VNN1	1.387609426	0.018322947	1.82614616	0.002860491
DYSF	1.380334025	0.000240843	1.38766132	0.003343979
MS4A4A	1.343842261	0.036359047	1.59240882	0.000535323
SLC22A4	1.339679498	0.000131462	1.57913684	7.25E-05
SLC25A37	1.311678316	0.001876504	1.093944	0.004596929
HCAR3	1.282670291	0.017589879	1.40054834	0.006558044
RAB20	1.267457005	0.000593788	1.0664515	0.014955308
SLPI	1.216777783	0.008732896	1.13878499	0.009829437
PGLYRP1	1.214296158	0.02633062	1.4091965	0.006967278
SPI1	1.173638634	0.000648156	1.26980533	0.008991834
CD14	1.160085184	0.00047528	1.04027166	0.00959378
PGD	1.159103617	0.000991555	1.28643817	0.007457779
S100A9	1.152294591	1.49E-05	1.25224368	0.00194674
LILRA5	1.142616414	9.05E-05	1.64694234	0.009424013
PLAUR	1.13704528	6.79E-05	1.13836929	0.000468437
ZYX	1.123336273	0.000164154	1.13635834	0.011079268
TIMP1	1.116578007	0.000172174	1.1271795	0.010817801
FOLR3	1.047931511	0.037703653	1.53888832	0.004675327
RNASE3	1.040091939	0.019168376	1.26981037	0.006569719
CCR1	1.009959825	0.011014418	1.03113099	0.017080198
CD79A	-1.100323819	0.000253237	-1.25472054	0.012659851
PTPRK	-1.140138272	8.35E-06	-1.06173	0.000467041
KLRF1	-1.396682363	0.003592261	-1.19328104	0.002954237
CD79B	-1.438267028	0.000244429	1.02734351	0.019134191
TRAF5	-1.547617803	3.06E-05	-1.30228767	0.003582083
TCL1A	-1.835177218	0.0002124	-1.13118967	0.02285283

Abbreviations: FC, fold change.

PPI Network Analysis of Common DEGs

After eliminating the isolated nodes, the PPI network was constructed with 25 nodes and 39 edges, including 23 up-regulated genes and two down-regulated genes, as shown in Figure 4A. The genes with degree ≥ 3 were deemed as hub genes in the PPI network, including SPI1 connecting seven nodes, S100A12 connecting seven nodes, S100A9 connecting five nodes, CD79A connecting four nodes, and CD79B connecting three nodes (Figure 4B).

Construction of a MiRNA-TF-mRNA Regulatory Network

A miRNA-TF-mRNA regulatory network was constructed, which consisted of 111 nodes and 105 edges, including 81 target miRNAs, 18 transcription factors, and 12 mRNAs (Figure 5). The result showed that SPI1 could target miR-361-5p, miR-155-5p, and miR-339-5p in the progression of IE.

Drug-Gene Network Analysis

In the drug-gene network, 90 drug-gene pairs were acquired, including 18 CDEGs (including SLPI, CD79B, S100A9, S100A12, and ANPEP) and 72 drugs (Figure 6). S100A9 could interact with methyldopa (Matola, Ahmedabad, India) and S100A12 could interact with rimegepant (New Haven, CT, USA), which might be the target of treatment of IE, but the specific mechanism is still unclear.

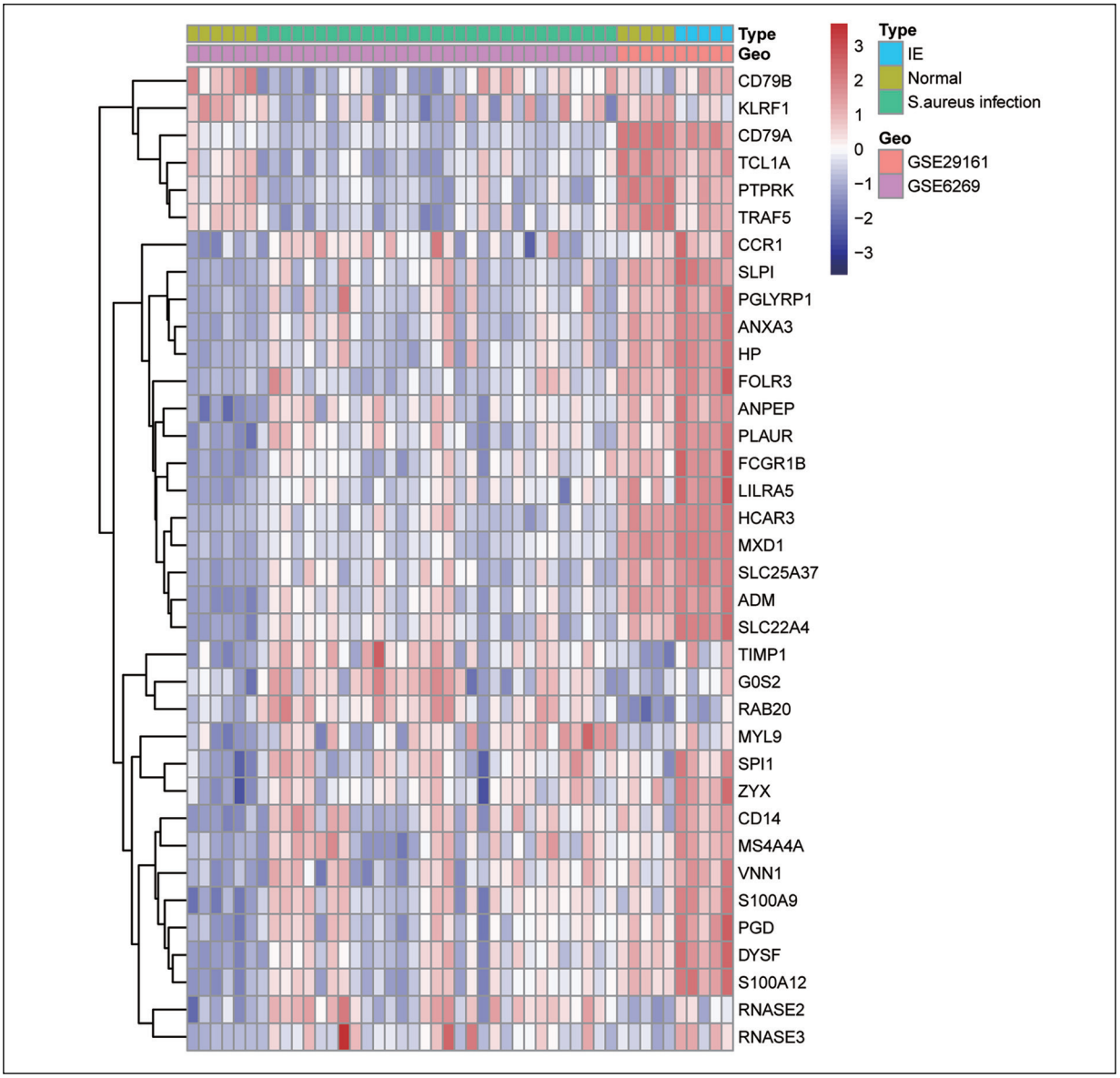

Figure 2. Heat map of the common DEGs. Each row represents the DEGs, and each column represents one of the samples of normal, IE, or *S. aureus* infection. The red and blue color represent upregulated and downregulated DEGs, respectively. Abbreviations: DEGs, differentially expressed genes; FC, fold change.

Discussion

Infective endocarditis is the inflammation of the endocardium and valves of the heart chambers caused by different pathogens including various bacteria, fungi, and viruses[22], among which, *S. aureus* is one of the most important causative agents[23]. However, the ability to diagnose *S. aureus*-induced IE in the early stage is still poor, and hence, it is urgent and essential to uncover specific genes and pathways in the progression of *S. aureus*-induced IE.

Two independent datasets were chosen in the current study. As the GSE6269 dataset included multiple categories of infectious patients and normal samples, we selected *S. aureus*-infected patients from this dataset. The GSE29161 was a novel dataset that had not previously been explored and included five IE patients and five healthy controls. Overall, 201 and 741 DEGs were respectively identified from the GSE6269 and GSE29161 databases. With the intersection of the DEGs, we discovered 36 CDEGs (30 up-regulated and six down-regulated), which meant

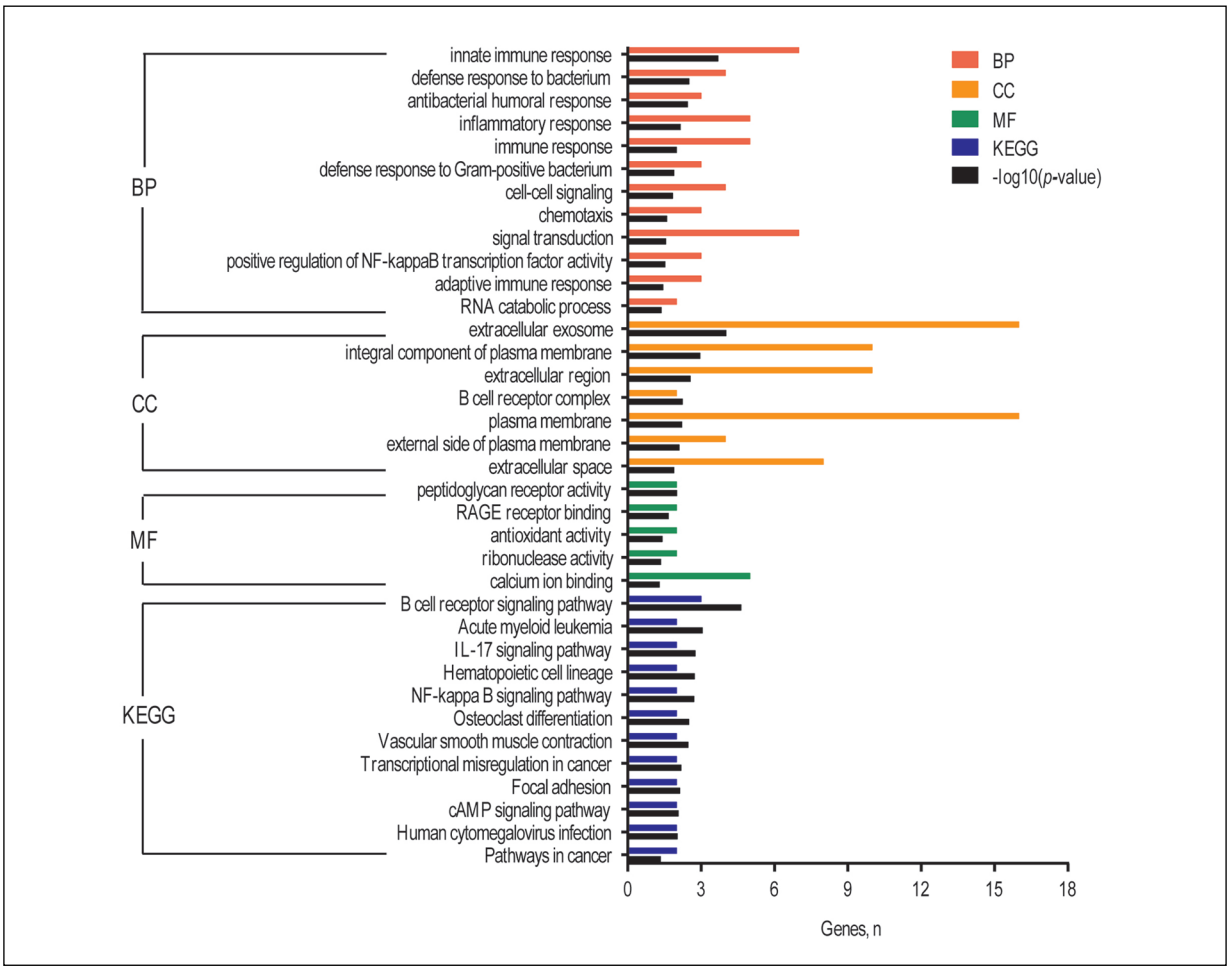

Figure 3. GO and KEGG analyses of the common DEGs. The vertical and horizontal axes represent GO term and -log10 (*p*-value) of the corresponding GO term, respectively. Different colors present main categories of the GO terms – BP, CC, and MF – as well as the KEGG pathway. Abbreviations: DEGs, differentially expressed genes; GO, Gene Ontology; MF, molecular function; CC, cellular component; BP, biological process; KEGG, Kyoto Encyclopedia of Genes and Genomes.

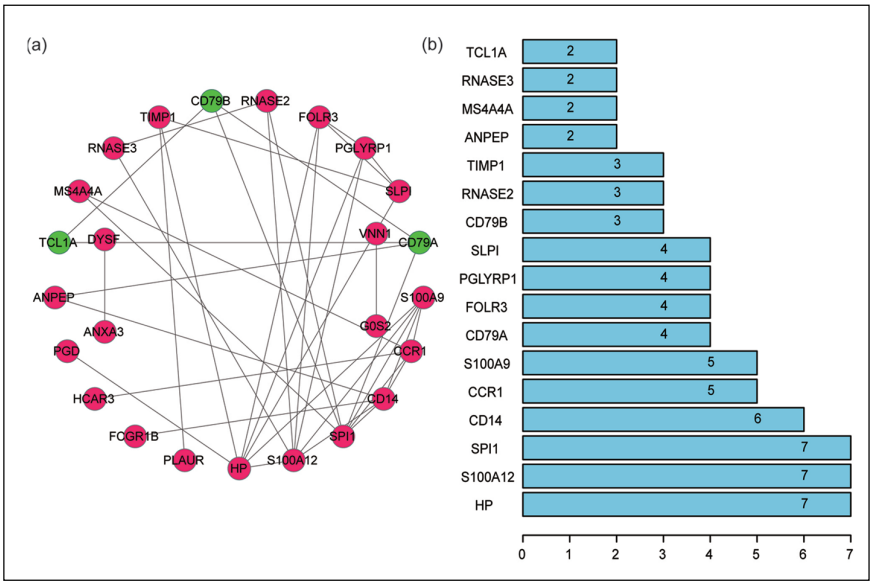

Figure 4. PPI network and histograms of core proteins of common DEGs. **A,** The red nodes and green nodes represent up-regulated genes and down-regulated genes, respectively. **B,** Abscissa shows the gene name; ordinate indicates the number of contiguous genes; and height represents the number of gene connections. Abbreviations: PPI, protein-protein interaction; DEGs, differentially expressed genes.

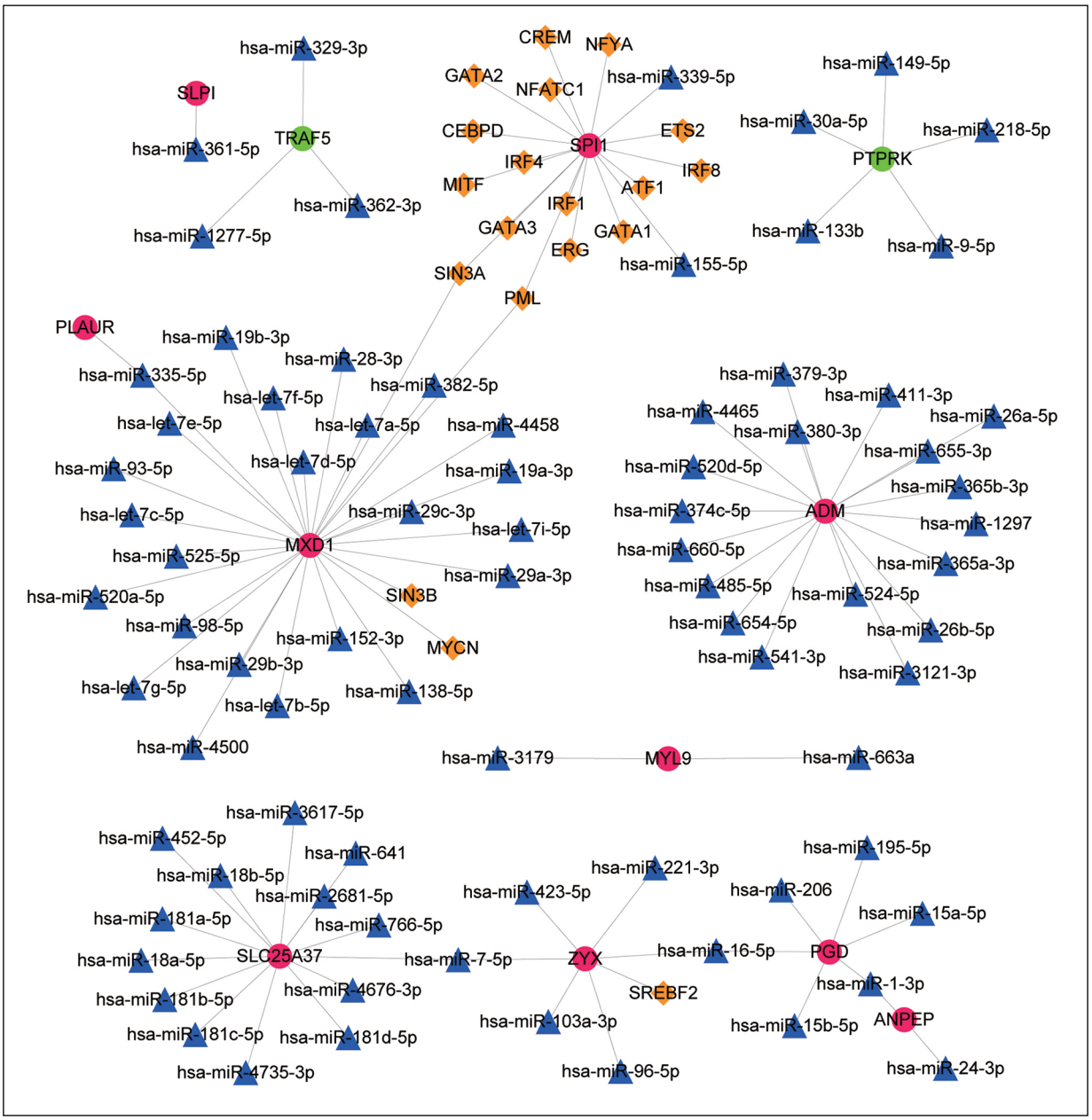

Figure 5. MiRNA-TF-mRNA regulatory network. Red circles, green circles, blue triangles, and brown diamonds represent upregulated genes, downregulated genes, miRNAs, and TFs, respectively. Abbreviations: miRNAs, microRNAs; TF, transcription factor; mRNA, messenger RNA.

that these genes were associated with IE patients infected with *S. aureus*. All these CDEGs were annotated subjected to functional enrichment analyses. With the construction of the PPI network, hub CDEGs including HP, S100A12, SPI1, CD14, CCR1, S100A9, CD79a, FOLR3, PGLYRP1, SLP1, CD79b, RNASE2, and TIMP1 were mapped (nodes ≥ 3).

Our functional enrichment analyses showed that the B-cell receptor signaling pathway played a crucial role in *S. aureus*-infected IE. The pivotal molecule in this process included CD79a and CD79b. CD79 consists of CD79a and CD79b and plays an important role in initiating the signal transduction cascade triggered by antigen binding to the B-cell antigen receptor[24]. CD79a and CD79b were found to be vital in the progression of lymphoma[25] and endometriosis[26]. With the consideration of PPI network, we discovered that porcine PU.1 gene (SPI1) could interact

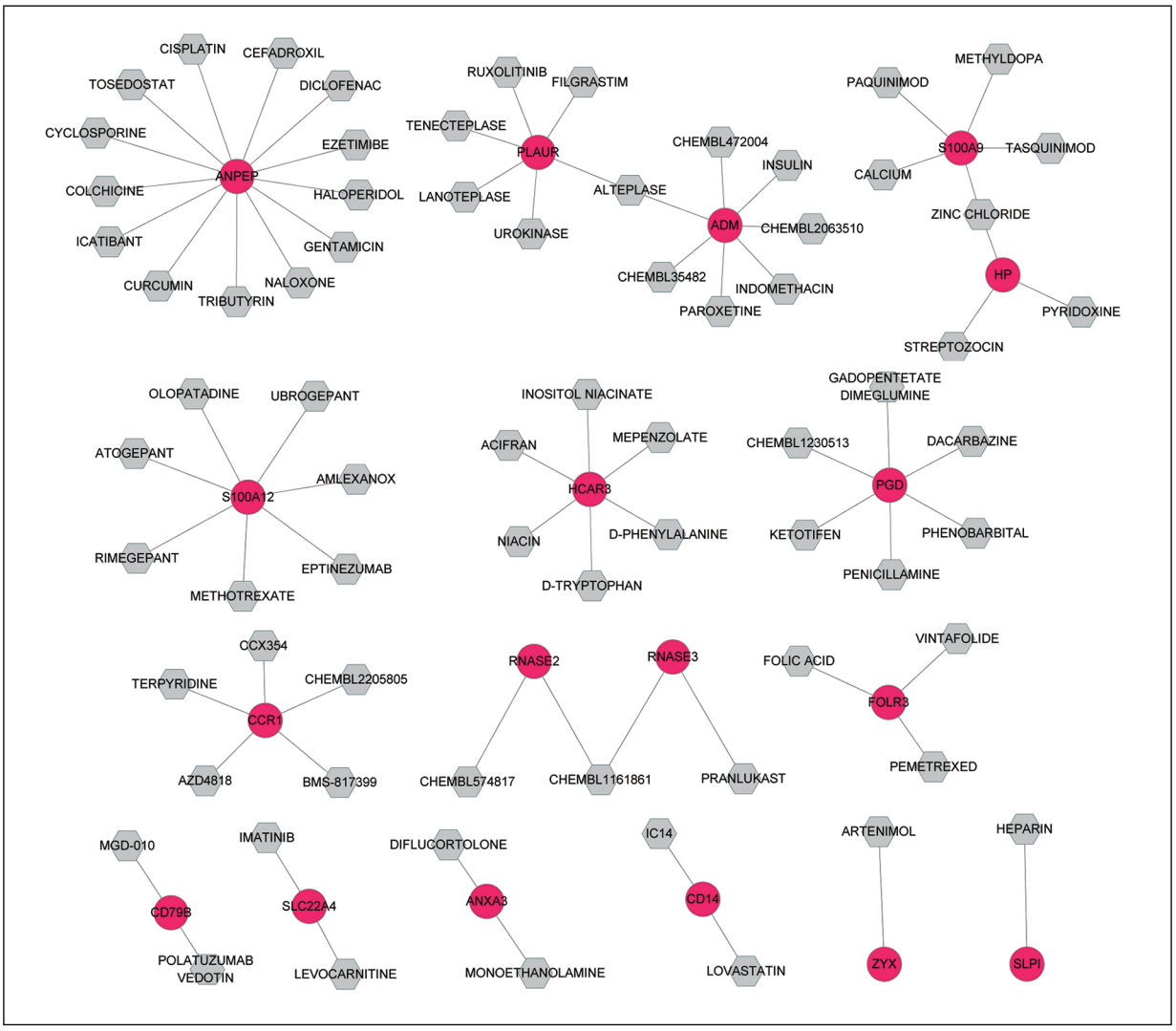

Figure 6. Drug-gene network. Red nodes and gray rectangles represent upregulated genes and drugs, respectively.

with CD79a and CD79b. Niu et al[27] showed that SPI1 may be a transcription factor to regulate genes in the development of heart failure from acute myocardial infarction (AMI). In addition, the miRNA-TF-mRNA network was established; miR361-5p, miR155-5p, and miR339-5p were predicted to be connected with SPI1. Researchers found that ischemia-reperfusion injury in the heart and brain could be alleviated by the up-regulation of miR361[28,29]. MiR339 was reported to inhibit cell proliferation and invasion in hepatocellular carcinoma[30]. Broad evidence showed that miR155 might work in the heart, including enhancing oxidative damage in endothelial cells preprocessed with H2O2[31], promoting apoptosis after AMI[32], and impairing cardiac function in patients with post-MI cardiac failure[33]. The relationship between miR155 and infection has also been reported. Shen et al[34] discovered that down-regulation of miR155 might inhibit inflammatory response in influenza A virus-affected human pulmonary microvascular endothelial cells. To our knowledge, this study was the first to reveal that CD79a, CD79b, and SPI1 could interact with each other, and that miR361-5p, miR155-5p, and miR339-5p might target SPI1 in the pathogenesis of *S. aureus*-induced IE.

Interestingly, we observed another two homologous molecules—S100 Calcium Binding Protein A9 (S100A9) and S100 Calcium Binding Protein A12 (S100A12)—with regard to the hub genes in the PPI network. They are both calcium- and zinc-binding proteins that belong to the family of S100 proteins. Their prominent roles in the regu-

lation of inflammatory and immune response have been demonstrated by comprehensive data, which was consistent with our enrichment analyses. Banupriya et al[35] discovered zinc supplementation by targeting S100A9 expression could reduce inflammation in neonates with sepsis. Czapski et al[36] found that the level of S100A9 expression was higher in the brains of subjects with Alzheimer's disease, indicating that the immune response was activated. Müller et al[37] reported that serum alarmin S100A8/S100A9 levels could be potential biomarkers in myocarditis. The reviews of S100A12 showed that it was likely a potential biomarker of therapeutic efficacy and disease progression in coronary heart disease[38]. Shah et al[39] found that S100A9 and S100A12 played key immune response roles in inflammatory disorders of the cardiovascular system. Taking the drug-gene network into consideration, we speculated several drugs targeting S100A9 and S100A12 in treating *S. aureus*-induced IE, including methyldopa targeting S100A9, an antihypertensive drug, and rimegepant targeting S100A12, a migraine drug. However, more evidence is still required for confirming the function of these drugs in treating AF. Until now, few research studies have investigated the specific mechanisms of the S100 protein family and *S. aureus*-induced IE. Moreover, further laboratory studies are essential to confirm the observations of key genes and pathways in *S. aureus*-induced IE.

Conclusions

Five pivotal genes were hypothesized in IE caused by *S. aureus*, including CD79a, CD79b, SPI1, S100A9, and S100A12; of these, CD79a, CD79b, and SPI1 co-function by participating in the B-cell receptor signaling pathway, while S100A9 and S100A12 played crucial roles in the immune and inflammatory response. Our results have provided new perspectives for the early detection of *S. aureus*-induced IE.

Conflict of Interest

The Authors declare that they have no conflict of interests.

Funding

This work was supported by the grants from Applied Basic Research Project of Xuzhou to Defeng Pan (grant number: XM12B024).

References

1) Salem A, Azeez S, Stirrup J, Lawrence D, Ruparelia N. Streptococcus intermedius masquerading as fungal infective endocarditis. Br J Hosp Med (Lond) 2019; 80: 674-675.
2) Cahill TJ, Prendergast BD. Infective endocarditis. Lancet 2016; 387: 882-893.
3) Tascini C, Aimo A, Arzilli C, Sbrana F, Ripoli A, Ghiadoni L, Bertone C, Passino C, Attanasio V, Sozio E, Taddei E, Murri R, Fantoni M, Paciosi F, Francisci D, Pasticci MB, Pallotto C, Di Caprio G, Carozza A, Maffei S, Emdin M. Procalcitonin, white blood cell count and C-reactive protein as predictors of S. aureus infection and mortality in infective endocarditis. Int J Cardiol 2020; 301: 190-194.
4) Yee R, Cui P, Shi W, Feng J, Wang J, Zhang Y. Identification of a novel gene argJ involved in arginine biosynthesis critical for persister formation in Staphylococcus aureus. Discov Med 2020; 29: 65-77.
5) Mgbojikwe N, Jones SR, Leucker TM, Brotman DJ. Infective endocarditis: beyond the usual tests. Cleve Clin J Med 2019; 86: 559-567.
6) Razmi R, Magnusson P. [Management of infective endocarditis]. Lakartidningen 2019; 116: FEPZ.
7) Rowe SE, Wagner NJ, Li L, Beam JE, Wilkinson AD, Radlinski LC, Zhang Q, Miao EA, Conlon BP. Reactive oxygen species induce antibiotic tolerance during systemic Staphylococcus aureus infection. Nat Microbiol 2020; 5: 282-290.
8) Mirzaei R, Mohammadzadeh R, Mirzaei H, Sholeh M, Karampoor S, Abdi M, Alikhani MY, Kazemi S, Ahmadyousefi Y, Jalalifar S, Yousefimashouf R. Role of microRNAs in Staphylococcus aureus infection: Potential biomarkers and mechanism. IUBMB Life 2020; 72: 1856-1869.
9) Ranganathan N, Johnson R, Edwards AM. The general stress response of Staphylococcus aureus promotes tolerance of antibiotics and survival in whole human blood. Microbiology (Reading) 2020; 166: 1088-1094.
10) Tao Z, Shi A, Li R, Wang Y, Wang X, Zhao J. Microarray bioinformatics in cancer- a review. J BUON 2017; 22: 838-843.
11) Kulasingam V, Diamandis EP. Strategies for discovering novel cancer biomarkers through utilization of emerging technologies. Nat Clin Pract Oncol 2008; 5: 588-599.
12) Clough E, Barrett T. The Gene Expression Omnibus Database. Methods Mol Biol 2016; 1418: 93-110.
13) Ritchie ME, Phipson B, Wu D, Hu Y, Law CW, Shi W, Smyth GK. Limma powers differential expression analyses for RNA-sequencing and microarray studies. Nucleic Acids Res 2015; 43: e47.

14) Jiao X, Sherman BT, Huang da W, Stephens R, Baseler MW, Lane HC, Lempicki RA. DAVID-WS: a stateful web service to facilitate gene/protein list analysis. Bioinformatics 2012; 28: 1805-1806.

15) Wu J, Mao X, Cai T, Luo J, Wei L. KOBAS server: a web-based platform for automated annotation and pathway identification. Nucleic Acids Res 2006; 34: W720-724.

16) Franceschini A, Szklarczyk D, Frankild S, Kuhn M, Simonovic M, Roth A, Lin J, Minguez P, Bork P, von Mering C, Jensen LJ. STRING v9.1: protein-protein interaction networks, with increased coverage and integration. Nucleic Acids Res 2013; 41: D808-815.

17) Smoot ME, Ono K, Ruscheinski J, Wang PL, Ideker T. Cytoscape 2.8: new features for data integration and network visualization. Bioinformatics 2011; 27: 431-432.

18) Chou CH, Shrestha S, Yang CD, Chang NW, Lin YL, Liao KW, Huang WC, Sun TH, Tu SJ, Lee WH, Chiew MY, Tai CS, Wei TY, Tsai TR, Huang HT, Wang CY, Wu HY, Ho SY, Chen PR, Chuang CH, Hsieh PJ, Wu YS, Chen WL, Li MJ, Wu YC, Huang XY, Ng FL, Buddhakosai W, Huang PC, Lan KC, Huang CY, Weng SL, Cheng YN, Liang C, Hsu WL, Huang HD. miRTarBase update 2018: a resource for experimentally validated microRNA-target interactions. Nucleic Acids Res 2018; 46: D296-d302.

19) Li JH, Liu S, Zhou H, Qu LH, Yang JH. starBase v2.0: decoding miRNA-ceRNA, miRNA-ncRNA and protein-RNA interaction networks from large-scale CLIP-Seq data. Nucleic Acids Res 2014; 42: D92-97.

20) Chen EY, Tan CM, Kou Y, Duan Q, Wang Z, Meirelles GV, Clark NR, Ma'ayan A. Enrichr: interactive and collaborative HTML5 gene list enrichment analysis tool. BMC Bioinformatics 2013; 14: 128.

21) Cotto KC, Wagner AH, Feng YY, Kiwala S, Coffman AC, Spies G, Wollam A, Spies NC, Griffith OL, Griffith M. DGIdb 3.0: a redesign and expansion of the drug-gene interaction database. Nucleic Acids Res 2018; 46: D1068-d1073.

22) Franconieri F, Join-Lambert O, Creveuil C, Auzou M, Labombarda F, Aouba A, Verdon R, de La Blanchardière A. Rothia spp. infective endocarditis: A systematic literature review. Med Mal Infect 2020 Oct 22:S0399-077X(20)30761-7.

23) Speziale P, Pietrocola G. The multivalent role of fibronectin-binding proteins A and B (FnBPA and FnBPB) of Staphylococcus aureus in host infections. Front Microbiol 2020; 11: 2054.

24) Chu PG, Arber DA. CD79: a review. Appl Immunohistochem Mol Morphol 2001; 9: 97-106.

25) Yonese I, Takase H, Yoshimori M, Onozawa E, Tsuzura A, Miki T, Mochizuki M, Miura O, Arai A. CD79B mutations in primary vitreoretinal lymphoma: diagnostic and prognostic potential. Eur J Haematol 2019; 102: 191-196.

26) Jerman LF, Anderson L, Markham R, Hey-Cunningham AJ. The lymphatic system in endometriosis: a pilot study of endometrial-like cells and immune cell populations in lymph nodes associated with deep infiltrating bowel lesions. Reprod Sci 2020; 27: 977-987.

27) Niu X, Zhang J, Zhang L, Hou Y, Pu S, Chu A, Bai M, Zhang Z. Weighted gene co-expression network analysis identifies critical genes in the development of heart failure after acute myocardial infarction. Front Genet 2019; 10: 1214.

28) Bu X, Li D, Wang F, Sun Q, Zhang Z. Protective Role of astrocyte-derived exosomal microrna-361 in cerebral ischemic-reperfusion injury by regulating the AMPK/mTOR signaling pathway and targeting CTSB. Neuropsychiatr Dis Treat 2020; 16: 1863-1877.

29) Xie Y, Yao FL, Li X. MicroRNA-361 regulates apoptosis of cardiomyocytes after ischemic-reperfusion injury. Eur Rev Med Pharmacol Sci 2019; 23: 5413-5421.

30) Zeng H, Zheng J, Wen S, Luo J, Shao G, Zhang Y. MicroRNA-339 inhibits human hepatocellular carcinoma proliferation and invasion via targeting ZNF689. Drug Des Devel Ther 2019; 13: 435-445.

31) Chen H, Liu Gao MY, Zhang L, He FL, Shi YK, Pan XH, Wang H. MicroRNA-155 affects oxidative damage through regulating autophagy in endothelial cells. Oncol Lett 2019; 17: 2237-2243.

32) Guo J, Liu HB, Sun C, Yan XQ, Hu J, Yu J, Yuan Y, Du ZM. MicroRNA-155 promotes myocardial infarction-induced apoptosis by targeting rna-binding protein QKI. Oxid Med Cell Longev 2019; 2019: 4579806.

33) Zhang B, Li B, Qin F, Bai F, Sun C, Liu Q. Expression of serum microRNA-155 and its clinical importance in patients with heart failure after myocardial infarction. J Int Med Res 2019; 47: 6294-6302.

34) Shen SM, Jiang H, Zhao JN, Shi Y. Down-regulation of miR-155 inhibits inflammatory response in human pulmonary microvascular endothelial cells infected with influenza A virus by targeting sphingosine-1-phosphate receptor 1. Chin Med J (Engl) 2020; 133: 2429-2436.

35) Banupriya N, Bhat BV, Vickneshwaran V, Sridhar MG. Effect of zinc supplementation on relative expression of immune response genes in neonates with sepsis: a preliminary study. Indian J Med Res 2020; 152: 296-302.

36) Czapski GA, Zhao Y, Lukiw WJ, Strosznajder JB. Acute systemic inflammatory response alters transcription profile of genes related to immune response and Ca2+ homeostasis in hippocampus; relevance to neurodegenerative disorders. Int J Mol Sci 2020; 21: 7838.

37) Müller I, Vogl T, Kühl U, Krannich A, Banks A, Trippel T, Noutsias M, Maisel AS, van Linthout S, Tschöpe C. Serum alarmin S100A8/S100A9 lev-

els and its potential role as biomarker in myocarditis. ESC Heart Fail 2020; 7: 1442-1451.

38) Xiao X, Yang C, Qu SL, Shao YD, Zhou CY, Chao R, Huang L, Zhang C. S100 proteins in atherosclerosis. Clin Chim Acta 2020; 502: 293-304.

39) Shah RD, Xue C, Zhang H, Tuteja S, Li M, Reilly MP, Ferguson JF. Expression of calgranulin genes S100A8, S100A9 and S100A12 is modulated by n-3 PUFA during inflammation in adipose tissue and mononuclear cells. PLoS One 2017; 12: e0169614.